2011

Thermally activated transitions in a system of two single domain ferromagnetic particles

Dorin Cimpoesu

Alexandru Stancu

Ivo Kilk

Ching-Ray Chang

Leonard Spinu
University of New Orleans

Recommended Citation

J. Appl. Phys. 109, 07D339 (2011)

Thermally activated transitions in a system of two single domain ferromagnetic particles

Dorin Cimpoesu,[1,a)] Alexandru Stancu,[1,b)] Ivo Klik,[2,c)] Ching-Ray Chang,[2,d)] and Leonard Spinu[3]
[1]*Department of Physics, Al. I. Cuza University, Iasi 700506, Romania*
[2]*Department of Physics, National Taiwan University, Taipei, Taiwan 107*
[3]*Advanced Materials Research Institute (AMRI) and Department of Physics, University of New Orleans, New Orleans, Louisiana 70148, USA*

(Presented 17 November 2010; received 8 September 2010; accepted 14 December 2010; published online 8 April 2011)

Numerical simulations based on the stochastic Langevin equation are applied here to a system of two uniaxial single domain ferromagnetic particles with antiferromagnetic dipolar coupling. The hysteresis loops of a strongly coupled systems exhibit fully demagnetized, intermediate metastable configurations which separate the two fully saturated states. At small magnetostatic couplings, on the other hand, and at sufficiently weak damping, the intermediate metastable configuration becomes only partially demagnetized. This state cannot be associated with any single local minimum of the free energy function. © *2011 American Institute of Physics*.
[doi:10.1063/1.3562884]

INTRODUCTION

In perpendicular magnetic recording, one can use larger particles without increasing their anisotropy too much. However, interaction fields in this arrangement become quite high, and in the presence of thermal agitation also extremely complex.[1–3] We study here a pair of thermally activated particles with dipolar coupling of antiferromagnetic type. Such a study may provide a benchmark for more complex investigations and our result, indeed, does provide a new perspective on the effect of interactions in particulate media.

The thermally activated dynamics of a pair of parallel uniaxial particles were studied by Lyberatos and Chantrell[4] who applied Langevin equation simulations[5,6] to the special case of low energy barrier, high damping, when the line connecting the particles makes a bond angle $\beta = 0$ with the easy axes. The authors found in particular that the reversal by symmetric fanning, predicted by Chen *et al.*,[7] takes place only at strong coupling and high energy barrier.

In this paper, we apply Langevin equation simulations to the special case of antiferromagnetically (AFM) coupled identical uniaxial particles with bond angle $\beta = \pi/2$. We identify two qualitatively different reversal modes: a process which takes place only at low damping and low AFM coupling, and a process which takes place at high damping and strong coupling as well. We use the results of Chen *et al.*[7] who described the energy surface of two identical magnetostatically coupled uniaxial particles acted on by an external field parallel to the particles easy axes. For brevity we introduce here merely the coupling strength $\rho = M_s^2 V/(2Kr^3)$ where K is the anisotropy constant, V the activation volume, M_s the saturation magnetization, and r the distance between the particles. We also introduce the standard nucleation field $H_n = 2K/M_s$, and the reduced field $h = H/H_n$. The bond angle $\beta = \pi/2$ everywhere.

The analysis of Chen *et al.*[7] allowed Klik *et al.*[8,9] to write down a three level master equation for the occupation probabilities of the three distinct metastable configurations $\uparrow\uparrow$, $\uparrow\downarrow + \downarrow\uparrow$, and $\downarrow\downarrow$ of the system. At zero or sufficiently low applied field these metastable states represent four local minima on the free energy surface of the two-particle system. At the other extreme is the case of a very large applied field which allows the existence of only a single, fully magnetized state. The thermally activated transition rates between the metastable states are determined by barrier heights separating them. The prefactor of the thermal relaxation rate was taken to be constant, and all back-reversal processes[10] were excluded. The rate (master) equation yields the time dependent occupation probabilities of the three metastable states. At sufficiently small fields[9] it may schematically be represented by the diagram

$$\uparrow\uparrow \leftrightarrow \uparrow\downarrow + \downarrow\uparrow \leftrightarrow \downarrow\downarrow .$$

In the limit $\rho \to 0$ the three level master equation goes over to the free particle limit.

In order to describe the thermally activated dynamics of the two-particle system, we employ a Langevin stochastic equation of motion based on the standard Gilbert equation[11] augmented by a stochastic thermal field which is assumed to be a Gaussian random.[12] It is assumed that the fluctuating fields acting on the different magnetic moments are independent. We interpret this equation in the sense of Stratonovich,[13] and numerically integrate it using an implicit midpoint time-integration technique.[14] No temperature dependence of the anisotropy constant and saturation magnetization are taken into account.

The applied field driving the loop is $h(t) = h_{\max} \cos 2\pi ft$, where f is the sweep frequency of the field. In our simulations

[a)]Electronic mail: cdorin@uaic.ro.
[b)]Electronic mail: alstancu@uaic.ro.
[c)]Electronic mail: iklik@phys.ntu.edu.tw.
[d)]Electronic mail: crchang@phys.ntu.edu.tw.

$f = 1$MHz. Starting from the initial positive saturated state, we let the system evolve during a time interval $\Delta t = (2fN)^{-1}$, N being the number of desired points on a curve. The average of the magnetization over the mentioned temporal window is then computed. This involves many thousands of steps in the numerical integration, since we set the time-step to be around 1 psec. On a given time interval, a set of $N_r = 10^6$ stochastic realizations of the stochastic process has been performed, and their statistics have been calculated. Then the evolution of the system on the next time interval is computed, and so on, until the system reaches negative saturation. For each temporal window the mean normalized magnetic moment along the applied field is

$$m_z = \frac{1}{N_r}\sum_{i=1}^{N_r}\left(m_{1z}^{(i)} + m_{2z}^{(i)}\right),$$

where $m_{jz}^{(i)}$ is the average (over the temporal window) projection along the applied field of the magnetization of the j-th particle ($j = 1, 2$) in the i-th stochastic realization.

The probabilities (occupation numbers) n_l that the system finds in the $l-$th state ($l = 1, 2, 3$) are computed as

$$n_1 = \begin{cases} \dfrac{1}{N_r}\displaystyle\sum_{i=1}^{N_r}\left(\dfrac{m_{1z}^{(i)} + m_{2z}^{(i)}}{2}\right), & \text{if } m_{1z}^{(i)} \geq 0 \text{ and } m_{2z}^{(i)} \geq 0 \\ 0, & \text{otherwise} \end{cases},$$

$$n_2 = \begin{cases} \dfrac{1}{N_r}\displaystyle\sum_{i=1}^{N_r}\left(\dfrac{|m_{1z}^{(i)}| + |m_{2z}^{(i)}|}{2}\right), & \text{if } m_{1z}^{(i)} m_{2z}^{(i)} < 0 \\ 0, & \text{otherwise} \end{cases},$$

$$n_3 = \begin{cases} \dfrac{1}{N_r}\displaystyle\sum_{i=1}^{N_r}\left(\dfrac{|m_{1z}^{(i)}| + |m_{2z}^{(i)}|}{2}\right), & \text{if } m_{1z}^{(i)} < 0 \text{ and } m_{2z}^{(i)} < 0 \\ 0, & \text{otherwise} \end{cases}.$$

Here n_1 is the occupation probability of the saturated state $\uparrow\uparrow$, n_2 is the occupation probability of the two demagnetized configurations $\uparrow\downarrow + \downarrow\uparrow$, n_3 and is the occupation probability of the inversely saturated state $\downarrow\downarrow$.

In Fig. 1 we show the reduced mean magnetization m_z together with the occupation probability n_2. The reduced inverse temperature here is $q = KV/k_BT = 42$, where k_B is Boltzmann's constant, and T is temperature, and the reduced coupling strength $\rho = 0.4$. The figure is in accord with the predictions of the master equation formalism:[9] The initial saturated $\uparrow\uparrow$ state reverses under the action of the field and goes over into the demagnetized configuration $\uparrow\downarrow + \downarrow\uparrow$. This configuration is metastable, and exists with occupation probability $n_2 = 1$ over a finite interval of the reversing field h. On further field reversal the demagnetized state becomes unstable and gradually switches into the saturated state $\downarrow\downarrow$. It is interesting to note that the transition $\uparrow\uparrow \rightarrow \uparrow\downarrow + \downarrow\uparrow$ is very fast and virtually independent of the damping constant α, while the decay of the demagnetized state is slower, and strongly dependent on α. The fastest decay takes place here at $\alpha = 0.5$, and the decay slows down with both increasing and decreasing α in accordance with the thermal decay theory.[15]

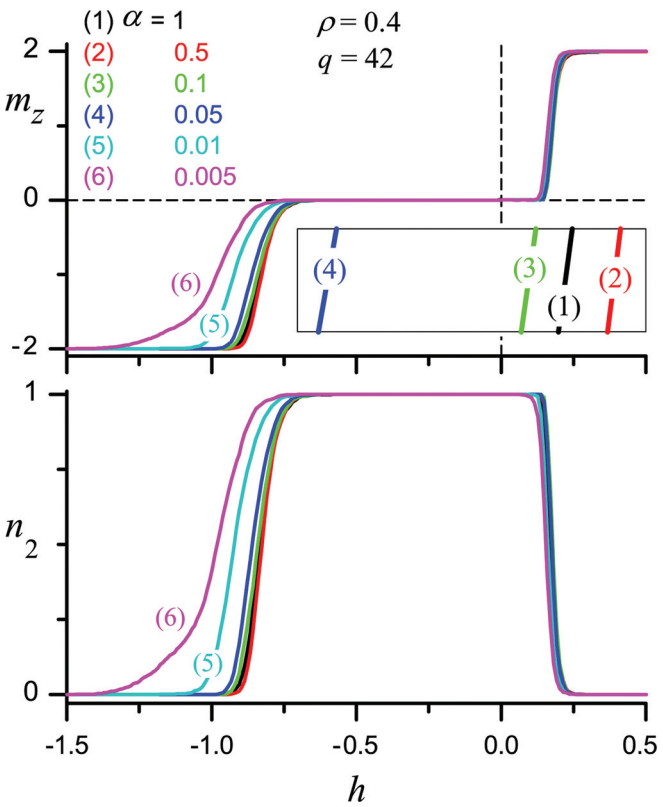

FIG. 1. (Color online) The reduced mean magnetization m_z along the driving field (top), and the occupation probability n_2 of the demagnetized state $\uparrow\downarrow + \downarrow\uparrow$ (bottom) vs the external biasing field $h(t) = h_{\max}\cos 2\pi\, ft$. The reduced inverse temperature $q = 42$, the driving field frequency $f = 1$MHz, the reduced coupling strength $\rho = 0.4$, and the dissipation constant $\alpha = 1, 0.5, 0.1, 0.05, 0.01$, and 0.005 as labeled. Inset (up): exploded view of m_z data for first four values of α; the curves follow in the same order also in the bottom panel.

The hysteresis loop of Fig. 1 is standard and presents no particular surprises. The situation changes, however, if the coupling strength is slightly decreased to $\rho = 0.2$, as shown in Fig. 2. In this case the domain of attraction of the demagnetized configuration is reduced, and the magnetization loops exhibit a partially demagnetized metastable state, which again exists over a finite interval of the external field. At large dissipative strength the magnitude of the nonzero metastable magnetization is quite small, but it increases appreciably at small values of α. We interpret this figure in terms of a reversal process in which the saturated state $\uparrow\uparrow$ decays into the demagnetized state and is either trapped there or continues immediately into the reverse saturated state $\downarrow\downarrow$. This picture is supported by an analysis of the random sojourn time which the system spends in the demagnetized state $\uparrow\downarrow + \downarrow\uparrow$. For $\rho = 0.4$ Fig. 3 shows the broad distribution of sojourn times associated with a thermally activated Markovian process. At $\rho = 0.2$, on the other hand, the sojourn times distribution has two peaks as is apparent form the plot of Fig. 4. In addition to the broad peak of overbarrier transitions there exists also a sharp, very narrow peak at very short sojourn times. This peak corresponds to a process during which the system is not trapped in the demagnetized state at all, but

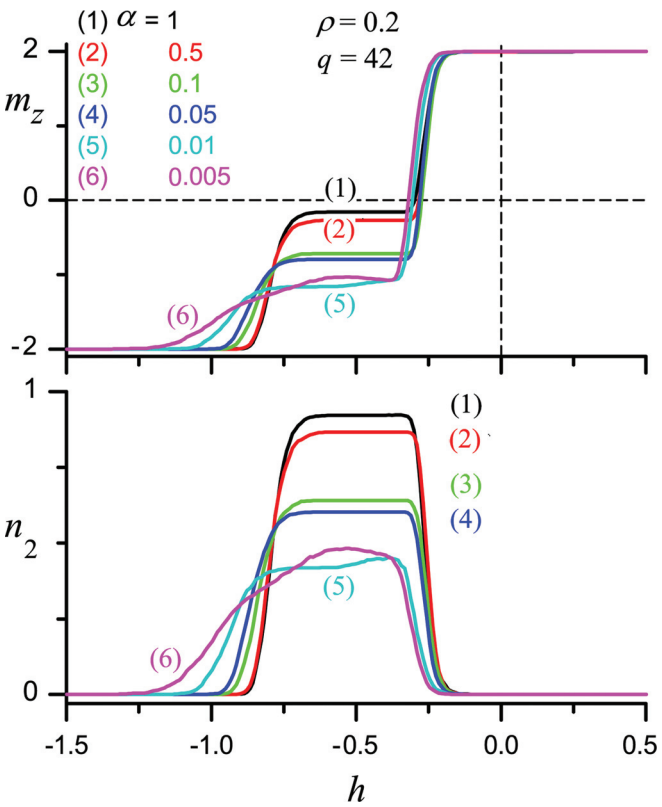

FIG. 2. (Color online) Same as Fig. 1, but with coupling strength $\rho = 0.2$.

proceeds directly, on a high energy trajectory, to the fully reversed configuration. The trapping probability is high at large α, where strong energy dissipation prevails, but small at small α, where the system may be thermally activated to a high energy at switching, and then continue to execute almost deterministic motion over a significant period of time. The partially demagnetized metastable states shown in Fig. 2 cannot be deduced from the free energy surface of the system, but are determined solely by the details of the dynamics. With increasing coupling strength these states gradually go over to fully demagnetized states, and they vanish altogether in the limit $\rho \to 0$ where no intermediate metastable state exists.

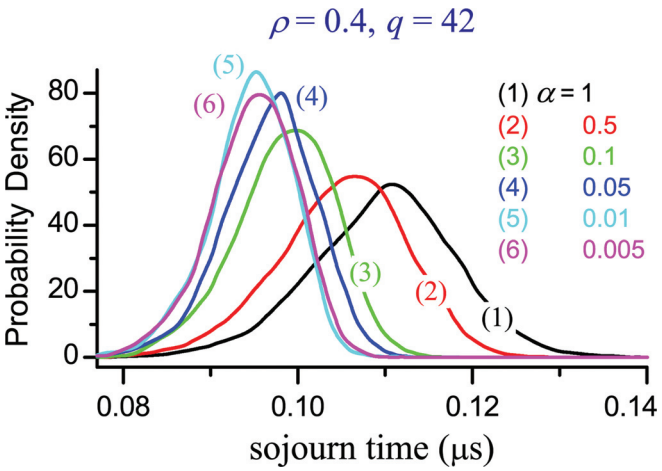

FIG. 3. (Color online) The sojourn times distribution in the demagnetized state $\uparrow\downarrow + \downarrow\uparrow$. The reduced inverse temperature $q = 42$, the reduced coupling strength $\rho = 0.4$, and the dissipation constant $\alpha = 1, 0.5, 0.1, 0.05, 0.01$, and 0.005 as labeled.

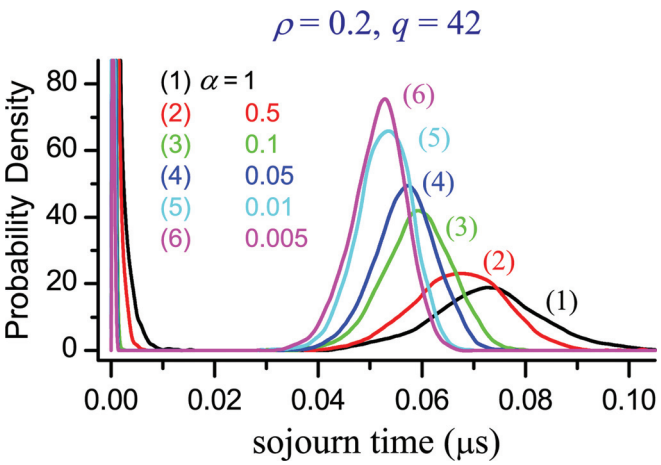

FIG. 4. (Color online) Same as Fig. 3 but with coupling strength $\rho = 0.2$.

ACKNOWLEDGMENTS

This work was partially supported by Romanian PNII 12-093 HIFI, PNII-RP3 Grant No. 9/1.07.2009, and by NSF under Grant No. ECCS-0902086. We also acknowledge Taiwan Grant No. NSC 98-2112-M-002-012-MY. A.S. also acknowledges the financial help from National Taiwan University.

[1]J. L. Dormann, D. Fiorani, and E. Tronc, Adv. Chem. Phys. **XCVIII**, 283 (1997).
[2]J. M. Shaw, S. E. Russek, T. Thomson, M. J. Donahue, B. D. Terris, O. Hellwig, E. Dobisz, and M. L. Schneider, Phys. Rev. B **78**, 024414 (2008).
[3]V. L. Safonov and H. N. Bertram, Phys. Rev. B **65**, 172417 (2002).
[4]A. Lyberatos and R. W. Chantrell, J. Appl. Phys. **73**, 6501 (1993).
[5]S. V. Titov, H. Kachkachi, Y. P. Kalmykov, and W. T. Coffey, Phys. Rev. B **72**, 134425 (2005).
[6]J. L. Garcia-Palacios and F. J. Lazaro, Phys. Rev. B **58**, 14937 (1998).
[7]W. Chen, S. Zhang, and H. N. Bertram, J. Appl. Phys. **71**, 5579 (1992).
[8]I. Klik and C. R. Chang, Phys. Rev. B **52**, 3540 (1995).
[9]I. Klik, C. R. Chang, and J. S. Yang, J. Appl. Phys. **76**, 6588 (1994).
[10]I. Klik and Y. D. Yao, J. Magn. Magn. Mat. **282**, 131 (2004).
[11]T. L. Gilbert, Phys. Rev. **100**, 1243 (1955);T. L. Gilbert, IEEE Trans. Magn. **40**, 3443 (2004).
[12]W. F. Brown, Jr., Phys. Rev. **130**, 1677 (1963).
[13]D. V. Berkov and N. L. Gorn, J. Phys.: Condens. Matter **14**, L281 (2002).
[14]M. d'Aquino, C. Serpico, G. Coppola, I. D. Mayergoyz, and G. Bertotti, J. Appl. Phys. **99**, 08B905 (2006).
[15]I. Klik and Y. D. Yao, J. Magn. Magn. Mat. **290**, 464 (2005).